

EFFECT OF THE INCORPORATION OF MESOPOROUS SILICA PARTICLES ON THE PHYSICAL PROPERTIES OF GELATINE GELS

Author: Laura Lidia García López. Directors: José Manuel Barat¹, Édgar Pérez Esteve¹

ABSTRACT

Mesoporous silica particles (MSP) appear to be a promising option as smart carriers of bioactive compounds in food. In this sense, it is important to understand the effect of the MSP on the physicochemical properties of the food in which they are added. In this work the effect of the addition of different MSP with and without functionalisation with N-(3-Trimethoxysilylpropyl) diethylenetriamine on the physical properties of gelatine gels (5% w/v) was studied by means of large deformations rheological essays and optical turbidity. All the MSP were characterised with the objective of correlate the particle features with its impact on the corresponding gel properties. Large deformation tests showed that the addition of MSP (both with and without the functionalisation) increased the stiffness (Young's modulus) of the gelatine gels. Furthermore, functionalised MSP showed a remarkable increase in the strength of the gels (increment of fracture stress) and a slight reduction of the brittleness of the gels (increment of fracture strain), in contrast with non-functionalised MSP which showed no effect on these two properties. Turbidity of the gels was also affected by the addition of all the MSP, presenting the particles that formed the smaller aggregates a higher contribution to turbidity.

Key words: MCM-41, UVM-7, SBA-15, gelatine, texture properties, turbidity, Young's modulus, fracture stress, fracture strain.

¹ Grupo de Investigación e Innovación Alimentaria (CUINA), Departamento de Tecnología de Alimentos, Universitat Politècnica de València, Camino de Vera s/n., 46022 Valencia, Spain.

RESUMEN

Las partículas mesoporosas de sílice (PMS) están emergiendo como una opción prometedora de encapsulamiento inteligente de compuestos bioactivos en alimentos. En este sentido, es importante entender su efecto en las propiedades fisicoquímicas del alimento al que están siendo incorporados. En este trabajo se ha estudiado el efecto de la adición de diferentes PMS funcionalizadas con N-(3-Trimetoxisililpropil)dielentriamina y sin funcionalizar sobre las propiedades físicas de geles de gelatina (5% p/v) a través de ensayos reológicos de gran deformación y turbidez óptica. Todas las PMS han sido caracterizadas con el objetivo de correlacionar sus características con su impacto en las propiedades del gel. Los ensayos de deformación muestran que la adición de todas las PMS (funcionalizadas y sin funcionalizar) aumentaron la rigidez de los geles (módulo de Young). Las PMS funcionalizadas presentaron, además, un notable incremento de la fuerza del gel (incremento del esfuerzo en la fractura) y una ligera disminución de la fragilidad del gel (incremento de la compresión en la fractura), a diferencia de las PMS no funcionalizadas, que no mostraron ningún efecto significativo. Finalmente, la turbidez de los geles se vio incrementada con la adición de las PMS, observándose una mayor contribución a la turbidez por parte de aquellas partículas que formaron agregados más pequeños.

Palabras clave: MCM-41, UVM-7, SBA-15, gelatina, turbidez, módulo de Young, esfuerzo en la fractura, deformación en la fractura.

RESUM

Les partícules mesoporoses de sílice (PMS) estan emergint com a una opció prometedora d'encapsulació intel·ligent de compostos actius en aliments. En aquest sentit, és important entendre el seu efecte sobre les propietats fisicoquímiques de l'aliment al qual són incorporades. En aquest treball s'ha estudiat l'efecte de l'addició de diferents partícules mesoporoses de sílice (PMS) funcionalitzades i sense funcionalitzar amb N-(3-Trimetoxisililpropil)dielentriamina sobre les propietats físiques de gels de gelatina (5% p/v) per mitjà d'assajos reològics de gran deformació i terbolesa òptica. Totes les PMS van ser caracteritzades amb l'objectiu de correlacionar les seues característiques amb el seu impacte en les propietats del gel al qual s'addicionen. Els assajos de deformació mostren que l'addició de totes les PMS (funcionalitzades i sense funcionalitzar) augmenten la rigidesa dels gels (mòdul de Young). Les PMS funcionalitzades presentaren un notable increment en la forà del gel (esforç en la fractura), i una lleugera disminució en la fragilitat del gel (increment de la compressió en la fractura), a diferència de les PMS no funcionalitzades, que no van mostrar cap efecte significatiu. Finalment, la terbolesa dels gels va incrementar a causa de l'addició de les PMS, tenint una major contribució a la terbolesa aquelles partícules que formen agregats de menor tamany.

Paraules clau: MCM-41, Hollow Silica, UVM-7, SBA-15, gelatina, propietats texturals, terbolesa, mòdul de Young, esforç en la fractura, deformació en la fractura.

INTRODUCTION

1. Mesoporous materials

In the last years, mesoporous silica particles (MSP) have been the focus of a great deal of attention in various life sciences fields such as medicine, pharmacy, agriculture and food technology due to their great potential in providing novel and improved solutions to many grand challenges in all these areas (Pérez-Esteve et al., 2013).

Their unique properties such as an ordered and uniform pore network, an adjustable pore size (from 2.0 nm to 50 nm), a high surface area ($>700 \text{ m}^2\text{g}^{-1}$) (Rouquerol et al., 1994; Trewyn et al., 2007; Vallet-Regí et al., 2007) as well as high stability (due to the thermal resistance and chemical inertness of the silica) and high biocompatibility (Jaganathan and Godin, 2012; Nandiyanto et al., 2009; Mamaeva et al., 2013) have favoured the development of biomedical applications related with the encapsulation of bioactive molecules inside its voids.

Within the MSP family, MCM-41 both in the nanosize (Agostini et al., 2012) and in the microsize (Climent et al., 2009), are the most studied and applied. However, lately, other MSP with different shape and porous systems have been described as molecule carriers: SBA-15 (Xu et al., 2010) and UVM-7 (Comes et al., 2009). These particles share a composition based in SiO_2 , a mesostructure, and the presence of silanol (SiOH) groups on their surface. They differ from each other in the particle size and shape, porous size and volume, the specific surface area and the density of silanol groups which provides different surface charge.

MSP are synthesized using assemblies of surfactants and block-copolymers as soft templates. Then, a source of silica is added, which condenses over the template to form the solid structure (Vallet-Regí et al., 2007). Figure 1 shows a scheme of this process.

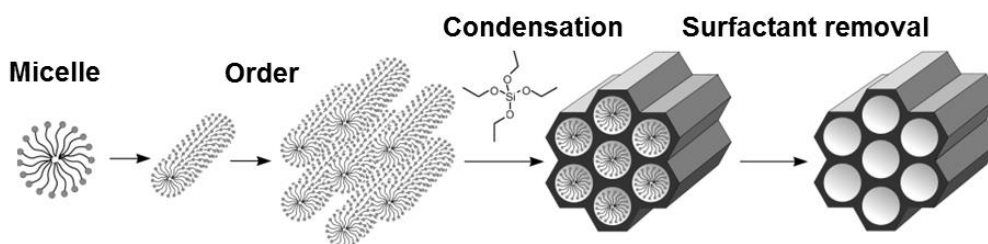


FIGURE 1. Scheme of the synthesis of a mesoporous silica material

2. Functionalised mesoporous materials as smart delivery systems

One of the most interesting features of MSP is that they have a high density of silanol groups on their framework, which can be used to link other organic silanol groups generating the so-called organic-inorganic hybrid materials (Vallet-Regí et al., 2007). The latter has represented a milestone for MSP opening a new range of possibilities for using them as smart systems for controlled storage, delivery and release of substances in the human body.

The organic groups grafted to the surface of the pores can operate like molecular gates that allow the delivery of encapsulated molecules depending of the external conditions or stimuli. For this purpose, amine molecules, such as N-(3-Trimethoxysilylpropyl)diethylenetriamine (N3), are suitable yet simple groups that have been proved to be successful as molecular gates for controlled release of substances such as vitamin B2 (Bernardos et al., 2008) and vitamin B9 (Barat et al., 2011). Once anchored to the surface, MSP functionalised with amines will behave as pH-triggered systems for controlled release that will be closed at acid pH (stomach conditions) and open at neutral pH (intestine conditions).

This has gathered the attention of this research group to explore the use of MSP and MSP functionalised with amines as smart carriers and delivers of substances in foods. However, before considering MSP as carriers additives in food, other considerations should be taken into account, such as the innocuousness of these materials and their effect on the physicochemical properties of the food in which they are added.

On the one hand, recent studies have not reported any toxicological danger related with MSP. Potential hazard with MSP is not related with the nature of the material, since silica has been commonly used in food industry as a preservative and thinning agent. The potential hazard relies in the size of the material, due to the fact that materials on a sub-micron and micron scale possess characteristics that can impose their biological behaviours and thus, affecting the integrity of the body cells (Jaganathan and Godin, 2012). In this sense, gastrointestinal toxicology of MSP has been studied over the past years, finding insignificant toxicity in vitro essays, low toxicity in immune cells and no evidence of toxicity in vivo experiments. In addition, once they get to the intestine, these particles are excreted in a relatively short period of time (from one to several days) (Jaganathan and Godin, 2012; Mamaeva et al., 2013).

On the other hand, to our best knowledge, the effect of the incorporation of MSP on the physicochemical and sensorial properties of food systems has not been previously studied. In this research an attempt to start filling this gap is made by studying the effect of the incorporation of several of the most frequently employed MSP (with and without functionalisation with N3) in a structured food model system such as gelatine gel.

3. Gelatine as a food model system

Gelatine is an ingredient broadly used in the food industry because of its functional properties such as hydration, thickening, gelation, suspending and fat replacement (Lee et al., 2003). These properties make gelatine an important ingredient in the elaboration of an ample group of products like: meat analogues, fabricated fruits and vegetables, milk-based dessert gels, dessert syrups and toppings, meat or fish aspics, low fat foods, pet food, edible films, emulsions, coating and food texturisers (Lau et al., 2000; Yang et al., 2012). Furthermore, different kinds of foods can be categorised as emulsion-filled gels including products like set yoghurt, fresh cheese, dairy desserts and sausages (Sala et al., 2009).

From the chemical point of view, gelatine is a derived protein produced from partial hydrolysis of protein collagen (Lee et al., 2003). It is a heterogeneous mixture of water-soluble proteins of high average molecular weight present in collagen. Thermal reversible gels of gelatine are obtained by heating an aqueous solution of gelatine (superior to 1%) at temperatures superior to 60°C and cooling. During heating, hot water denatures the triple-helical structure into individual soluble chains. After cooling, a physical gelation occurs due to the conformational transition of gelatine chains from coil to triple helixes segments, providing a cross-linked network (Karim & Bhat, 2008).

Gelatine forms soft, flexible and elastic gels (Lee et al., 2003). Properties of these gels, such as texture and strength are dependent on the gelatine concentration, pH, aging time (Lau et al., 2000; Kuijpers et al., 1999) and the incorporation of different molecules to the matrix (known as fillers) during the gelation process. These molecules modify gelatine properties in a greater or lesser extent depending on the physicochemical properties of the matrix and the filler, mass ratio between matrix and filler, particle size and interaction between the matrix and the filler components (Sala et al, 2009; Vaia and Wagner, 2004).

It has been reported that silanol groups from silicate species and amino groups are able to establish covalent bonding with the amino and carboxylic groups of the gelatine (Coradin et al., 2004; Lunqvist et al, 2008). Thus, this interaction could modify physical properties of the gels, attributes relevant to technology processes and to human texture perception and oral processing (van Vliet et al., 2009).

4. Scope of the thesis

The scope of the present thesis was to investigate the effect of the incorporation of the most employed MSP with and without functionalisation with N-(3-Trimethoxysilylpropyl)diethylenetriamine on the physical properties of gelatine gels (5% w/v) by means of large deformations rheological essays and optical turbidity determinations.

MATERIALS AND METHODS

1. Materials

The chemicals tetraethylorthosilicate (TEOS), n-cetyltrimethylammonium bromide (CTABr), Pluronic P123 (P123), triethanolamine (TEAH₃), N-(3-Trimethoxysilylpropyl)diethylenetriamine, sodium hydroxide (NaOH) and chloride acid (HCl) were provided by Sigma. Gelatine from porcine skin, type A, 300 Bloom, average molecular weight from 50-100 kDa and isoelectric point $pI=7.0-9.0$ was also provided by Sigma.

2. Methods

2.1 MESOPOROUS SILICA PARTICLES SYNTHESIS AND CHARACTERISATION

2.1.1 MESOPOROUS SILICA PARTICLES SYNTHESIS

Synthesis of Microparticulated MCM-41 was carried out following the so-called “atran route”, using CTABr as the structure-directing agent and a molar ratio fixed to 7TEAH₃:2TEOS:0.52CTABr:0.5NaOH:180H₂O. The procedure consisted in adding CTABr to a solution of TEAH₃ and NaOH containing TEOS at 118°C. After dissolving CTABr in the liquor, water was slowly added with vigorous stirring at 70°C to form a white suspension. This mixture was aged at room temperature overnight (Barat et al., 2011).

Nanoparticulated MCM-41 was synthesized using the following procedure: NaOH was added to the CTABr solution, followed by adjusting the solution temperature to 95 °C. TEOS was then added dropwise to the surfactant solution. The mixture was allowed to stir for 3 h to give a white precipitate (Bernardos et al., 2011).

UVM-7 was synthesised using, once again, the “atran route”. The molar ratio of the reagents in the mother liquor was fixed at TEAH₃:TEOS:CTABr:H₂O 7:2:0.52:180. The TEOS/TEAH₃ mixture was heated to 120°C until no elimination of ethanol was observed. The mixture was cooled to 90°C and the CTABr was added gradually in small portions, followed by water. The mixture was aged for 24h (Comes et al., 2009).

The SBA-15 sample was synthesized using P123 as the structure-directing agent with the reactant molar ratios: 0.017P123:1.0TEOS:6HCl:196H₂O. The preparation was carried mixing an aqueous solution of P123 with HCl solution, and stirring for 2 h, after which the silica source, TEOS, was added. This final mixture was stirred for a further 20 h (Zhao et al., 1988)

After the synthesis, the different solids were recovered, washed with deionised water, and air-dried at room temperature. The as-synthesized solids were calcined at 550°C using an oxidant atmosphere for 5h in order to remove the template phase.

2.1.2 MSP FUNCTIONALISATION

Each of the particles was functionalised with N-(3-Trimethoxysilylpropyl) diethylenetriamine. In a typical synthesis 1.00g of the different MSP were suspended in 40 mL of acetonitrile and an excess of the amine (4.3mL, 15.0 mmol) was added. The final mixtures were stirred for 5.5h at room temperature. Finally, the solids were filtered off, washed with 30mL of deionised water, and dried at room temperature.

2.1.3 PARTICLE SIZE AND MORPHOLOGY CHARACTERISATION

The morphology of single particles was determined via TEM (Hitachi, H-7650 operating at an acceleration voltage of 80 kV). The single particle size for each kind of particles was estimated by averaging 50 particle sizes measured by the size measurement tool of the TEM software.

Pore size, volume and the surface area were measured by porosimetry using N₂ adsorption-desorption isotherms. The isotherms were recorded with a Micrometrics ASAP2010 automated sorption analyzer. The samples were degassed at 120 °C in vacuum overnight. The specific surface areas were calculated from the adsorption data in the low pressure range using the BET model. Pore size was determined following the BJH method.

Moreover, the size distribution of these particle dispersions was measured with a Malvern Mastersizer 2000 (Malvern, UK) combining information from simple light scattering (LS) and polarization intensity differential scattering (PIDS). For data evaluation, an optical model based on the Mie theory was created using the instrumental software assuming 1.45 as the real and 0 as the imaginary part of the refractive index of the particles.

2.1.4 ZETA POTENTIAL MEASUREMENTS

Zeta potential (ζ) of the silica particles was measured at 25°C in a Zetasizer Nano ZS equipment (Malvern Instruments, UK). Samples were prepared at concentration of 1 mg in 1 mL of acetate buffer at pH 5.5. Before each measurement, each sample was sonicated for 2 minutes to preclude aggregation. Zeta potential distributions were obtained by averaging 5 measurements.

2.2 FILLED GELATINE GELS PREPARATION AND CHARACTERISATION

2.2.1 GELATINE GELS PREPARATION

Gelatine gels (5% w/v) were prepared with and without silica particles. For this purpose, a stock solution of gelatine (10% w/v) was prepared by allowing hydration for 2 h in sodium acetate buffer (pH 5.5) under gentle stirring at room temperature. The samples were subsequently dissolved by heating at 60°C for 30 min. Solutions of silica particles (0.01%, 0.05%, 0.1%, 0.5%, 0.75% and 1%) were prepared by mixing the particles with sodium acetate buffer (pH 5.5) and sonicating to reduce particle aggregates. To obtain control samples (samples without MSP) the stock solution was mixed 1:1 with acetate buffer. In the case

of filled gels, the gelatine solution was mixed with the selected solutions of silica particles at a ratio 1:1. After mixing, the samples were allowed to gel at 20°C in 20 mL plastic syringes (internal diameter 20 mm) coated with a thin film of paraffin oil for 22±2h before the texture analysis.

2.2.1 TURBIDITY MEASUREMENTS

For turbidity measurements each hot gelatine solution was poured into 1 cm plastic cuvettes and allowed to gel at 20°C. Turbidity (τ) was measured using a JASCO V-630 Spectrophotometer at 550 nm against acetate buffer and expressed as % of transmittance.

2.2.1 LARGE DEFORMATION EXPERIMENTS

For large deformation experiments, the gels were removed from the syringe and cut with a cutter (cylinder height: 20 mm). Uniaxial compression tests were performed using a texture analyzer (TA.XT.plus Texture Analyser, Stable Micro Systems, Godalming, Surrey, United Kingdom), and a 50 kg load cell equipped with a plate probe (diameter: 75 mm). For fracture essays, compression was exerted up to a strain of 90% with constant deformation speed of 1 mm/s. Eight replicates (2 pieces per specimen and 4 specimen per type of gel) were measured and the mean values for Young's modulus, fracture stress and strain were calculated. The pieces' absolute deformation was expressed as the Hencky's or true strain and true stress in the fracture. These parameters were calculated using the formulas in equation 1. (Peleg, 1987):

$$\epsilon_H = \int_{H_0}^H \frac{1}{H} dH = \ln \left(\frac{H}{H_0} \right) ; \sigma = \frac{F}{A} \left(\frac{H}{H_0} \right) \quad (1)$$

Where: ϵ_H = Hencky's or true strain; H = height of the sample at each moment (m), H_0 = initial height of the sample (m); σ = true stress; F = force (N); A = area of the sample (m²).

RESULTS AND DISCUSSIONS

1. Mesoporous silica particles characterisation

In order to correlate the characteristics of each prepared MSP with the properties exhibited by the filled gels, several analysis were carried out to determine the morphology and size of the particles. A structural analysis of the solids was done by transmission electron microscopy (TEM) as shown in Figure 2. Mesoporous structure was confirmed in all the MSP by the presence of typical porous channels with sizes ranging from 2.5 to 10nm, which is consistent with the definition of a mesoporous solid given by the IUPAC (Rouquerol, 1994).

The figure also shows differences between each type of MSP, not only in particle size and morphology, but in porous size as well. Nanoparticulated MCM-41 exhibited spherical nanoparticles (figure 2a), SBA-15 showed an elongated, cylindrical-shaped particles (figure 2b), while Microparticulated MCM-41 presented irregular-shaped agglomerated particles (figure 2c) and UVM-7 was displayed in form of clusters of pseudo spherical nanoparticles, forming a disordered system with small mesopores and large void-pores (macropores) (figure 2d). These results are similar to previous reports of the morphology and size of the MSP (Bernardos et al., 2008; Bernardos et al., 2011; Cabero et al., 2012; Charnay et al., 2004; Vallet-Regí et al., 2004; Vallet-Regí et al., 2007)

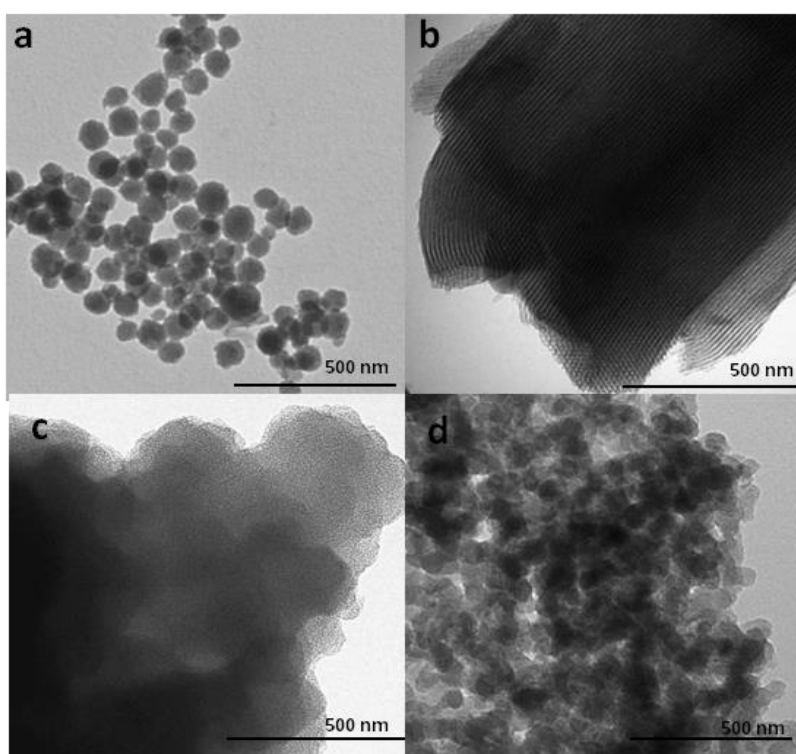


FIGURE 2. TEM images of Nanoparticulated MCM-41 (a), SBA-15 (b), Microparticulated MCM-41 (c) and UVM-7 (d).

To obtain more detailed information of the porous structure of the particles, a porosimetry analysis based on nitrogen adsorption-desorption was performed. Table 1 shows the specific surface area, pore volume and size of each MSP obtained from this analysis.

Consistent with TEM observations, Table 1 reveals that all MSP presented pore sizes ranging from 2.5 to 8 nm and that UVM-7 is the only particle that presented both mesopores and macropores. Nanoparticulated MCM-41, Microparticulated MCM-41 and UVM-7 displayed small pores diameters around 2.5-2.6nm, while SBA-15 exhibited the higher pore diameter, in the order of 8nm. In terms of pore volume, Microparticulated MCM-41 and SBA-15 exhibited the highest values followed by Nanoparticulated MCM-41 and UVM-7. Finally, Nanoparticulated MCM-41, Microparticulated MCM-41 and UVM-7 presented a similar surface area (roughly 1000 m²g⁻¹) whereas SBA-15 holds a significant lower value (approximately 600 m²g⁻¹).

TABLE 1. Pores characterisation of Nanoparticulated MCM-41 (N), Microparticulated MCM-41 (M), UVM-7 (U) and SBA-15 (S)

MSP	Mesopore			Macropore	
	Area (m ² /g)	Pore volume (c ³ /g)	Pore size (nm)	Pore volume (c ³ /g)	Pore size (nm)
N	1072.3	0.84	2.51		
M	1073.9	0.91	2.61		
U	919.2	0.75	2.65	1.10	54.80
S	648.9	0.92	7.89		

Pore size and volume, and surface area are particularly relevant in the incorporation and release of the molecules inside the MSP matrix. Pore size not only determines the size of the molecule that can be adsorbed into the structure (usually pore/molecule size ratio > 1 is needed), but also controls the molecule-release rate (Vallet-Regí et. al, 2007). In 2004, Horcajada and co-workers (2004) observed an evident increase of the release rate of ibuprofen with an increase of the pore size (from 40% to 60% of release by increasing 1nm the pore diameter). Pore volume is also important determining the maximum quantity of substance that can retain the matrix, while surface area becomes the more decisive factor for the amount of substance incorporated to the matrix, displaying significant changes in the adsorption by changing surface area from 700 to 1000 m²g⁻¹ (Vallet-Regí et. al, 2004). These observations suggest that the obtained Nanoparticulated MCM-41, Microparticulated MCM-41 and UVM-7 would present more potential for a higher substance adsorption than SBA-15, while SBA-15 would exhibit more potential for a higher substance release rate than the rest of the obtained MSP.

The former analyses were particularly useful to appreciate size and morphology of each individual nanoparticle. In order to observe the real arrangement formed by the particles (agglomerates) in the food matrix, size and zeta potential (with and without functionalisation) were determined in identical buffering conditions in which gelatines were prepared (acetate buffer, pH 5.5). Table 2 and Figure 3 show the results obtained.

TABLE 2. Size and zeta potential (Mean±SD) of Nanoparticulated MCM-41 (N), UVM-7 (U), Microparticulated MCM-41 (M), and SBA-15 (S) both in the solid state (TEM observation) and suspended in acetate buffer PH 5.5. Values with different letters in the same column are significantly different at p-value $p < 0.001$.

MSP	Non-functionalised	Non-functionalised in acetate buffer		Functionalised in acetate buffer	
	Single particle size (μm)	d(0,5) (μm)	Zeta potential (mV)	d(0,5) (μm)	Zeta potential (mV)
N	0.09±0.02 ^c	4.79±0.04 ^c	-13.3±1.1 ^a	0.86±0.01 ^b	57.3±2.6 ^a
U	0.67±0.03 ^b	6.19±0.04 ^b	-12.5±1.4 ^a	2.62±0.08 ^c	47.3±2.0 ^a
M	1.2±0.3 ^a	0.82±0.01 ^a	-30.1±0.6 ^c	0.55±0.00 ^a	75.5±2.8 ^c
S	1.3±0.2 ^a	0.78±0.00 ^a	-24.2±0.8 ^b	0.63±0.01 ^a	77.9±3.4 ^a

It is important to note that non-functionalised Nanoparticulated MCM-41 and UVM-7 agglomerates had a significant higher size than the individual nanoparticles observed on Fig 2. This is consistent with the agglomeration arrangement of these nanoparticles, also perceived in Fig. 2. Furthermore, zeta potential values of the MSP provides quite revealing results: first, it can be observed that all the particles changed from negatively to positively charged after the functionalisation, as a result of the amine groups attached on their framework, which is congruent with previous reports on amine functionalisation of MSP (Benhamou et al., 2013). More interesting, the amino groups not only change the nature of the charge, but also made the particles more colloiddally stable, with zeta potential values of all MSP away from the instability zone (from -30mv to 30mv).

This is confirmed by comparing agglomeration tendencies before and after the functionalisation: non-functionalised Nanoparticulated MCM-41 and UVM-7 showed agglomerates sizes in the order of the 4.8 and 6.2 μm , respectively, with zeta potential values within the instability zone, while, once functionalised, the size of the agglomerates decreased by 82% for Nanoparticulated MCM-41 and by 58% for UVM-7. Non-functionalised Microparticulated MCM-41 and SBA-15 presented zeta potential values bordering the stability zone, which allows to explain why the size of their agglomerates corresponded to one single particle size, contrary to Microparticulated MCM-41 and UVM-7. Decrease in the size of all the MSP agglomerates after functionalisation can be appreciated in Fig 3.

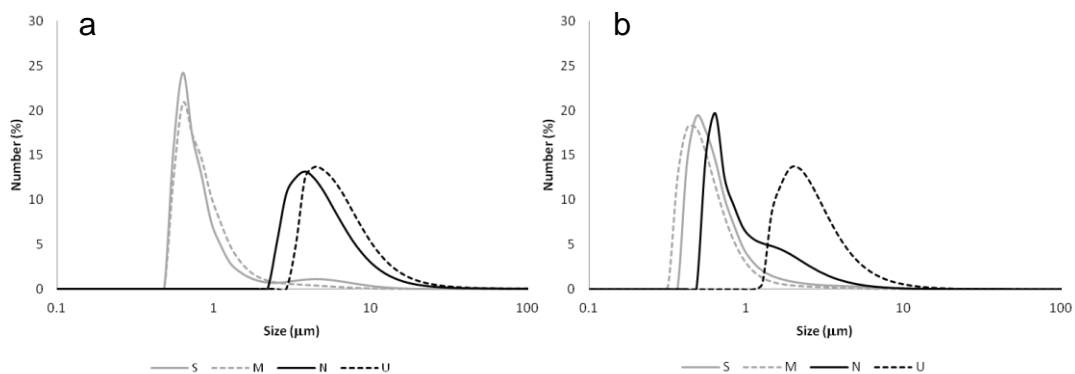


FIGURE 3. Size distribution of MSP in acetate buffer at pH 5.5. a) Non-functionalised MSP. b) Functionalised MSP. SBA-15 (S), Microparticulated, MCM-41 (M), Nanoparticulated MCM-41 (N) and UVM-7 (U).

2. Effect of the incorporation of MSP on the physical properties of gelatine gels

2.1 EFFECT ON TURBIDITY

Figure 4 shows the increase of turbidity (decrease of transmittance) of gelatine gels filled with the different MSP. It can be seen that turbidity decreased exponentially with increasing particle concentration at low concentration values (below 0.5% of MSP). This is consistent with light scattering theory, which states that for moderately dilute suspensions of particles, there is an exponential decrease in transmitted light with particle concentration (Gregory, 1998).

Figure 4 also shows that small particles (Microparticulated MCM-41 and SBA-15) increased the turbidity of the gels at very low concentrations, achieving 10% of transmittance at concentrations near 0.1%. However, large particles (Nanoparticulated MCM-41 and UVM-7) did not achieve the 10% of transmittance until they reached higher concentrations (near 0.5%). This can be explained by the Beer-Lambert Law, which enunciates that there is a logarithmic dependence between the number of particles per unit volume and the intensity of the transmitted light. In other words, higher number of particles will result in an exponential decrease of transmitted light. Since the gelatines are prepared based on mass concentration of the MSP, it is logical to assume that, for the same mass concentration, there would be more number of particles of the small size MSP (Microparticulated MCM-41 and SBA-15) than the large size MSP (Nanoparticulated MCM-41 and UVM-7) and therefore, the amount of transmitted light of the first ones will be lesser than the second ones, as seen in Fig.4.

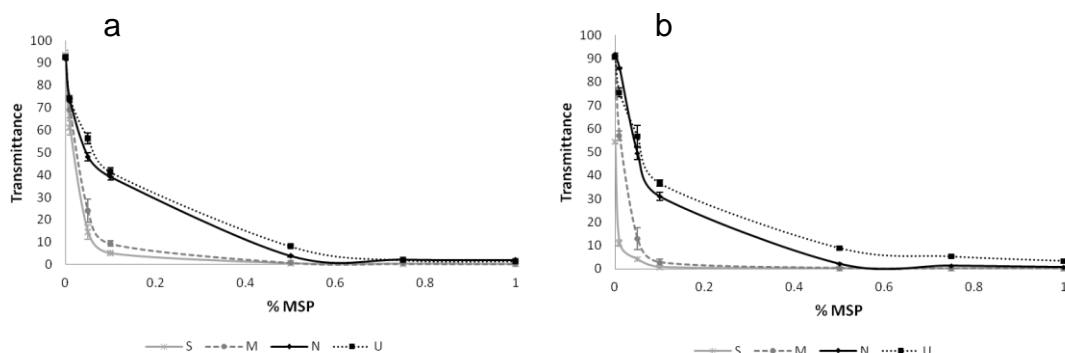


FIGURE 4. Transmittance at 550 nm of gelatine gels containing MSP at different concentrations. a) Non-functionalised MSP. b) Functionalised MSP. SBA-15 (S), Microparticulated MCM-41 (M), Nanoparticulated MCM-41 (N) and UVM-7 (U).

Finally, it can also be appreciated in Fig 4 that functionalised MSP had a superior contribution to turbidity than non-functionalised MSP. This can be the result of the evident size reduction of the particles due to the functionalisation (See Fig 3.) which, will lead to a higher number of functionalised particles than their respective counterpart, and hence a decrease in the transmitted light.

Another phenomenon that could be contributing to the increase in turbidity is the pore blockage of the MSP due to the functionalisation. In order to elaborate this hypothesis, first it is important to mention that mesoporous materials are expected to have a low refractive index because of their high degree of porosity (Haranath et al., 2010; Innocenzi and Malfatti, 2013; Maruo et al., 2008; Shubbert 2007), which will lead to a higher light transmittance. Before functionalisation, MSP exhibit open pores on their structure. Functionalisation, however, will result in the insertion of amine groups in the framework of the pores that, due to the acidic conditions of the medium (acetate buffer 5.5), will be protonated (See Table 2), tending to adopt a rigid-like conformation that will push them away to the pore openings, resulting in a pore blockage (Bernardos et al., 2008) that could contribute to inhibit the transmittance of light.

2.3 EFFECT ON THE LARGE DEFORMATION RHEOLOGICAL PROPERTIES

Young's modulus of the gels containing different MSP concentration is shown in Figure 5. The addition of both, functionalised and non-functionalised MSP, caused a moderate but significant increase on the Young's modulus of the gelatine gels.

Based on these results, it can be assumed that the incorporation of MSP made the gelatines stiffer, meaning that the filled gels presented a higher resistance to deflection. This is consistent with many studies on the improvement of the mechanical properties of polymeric matrixes where it is shown that the addition of rigid inorganic micro- and nano-particles (Silica, TiO₂, clay, etc.) enhanced the stiffness of the materials (Akihiro et al., 2013; Chrissafis et al., 2007; Fu et al., 2008; Tjon, 2006; Vaia and Wagner, 2004).

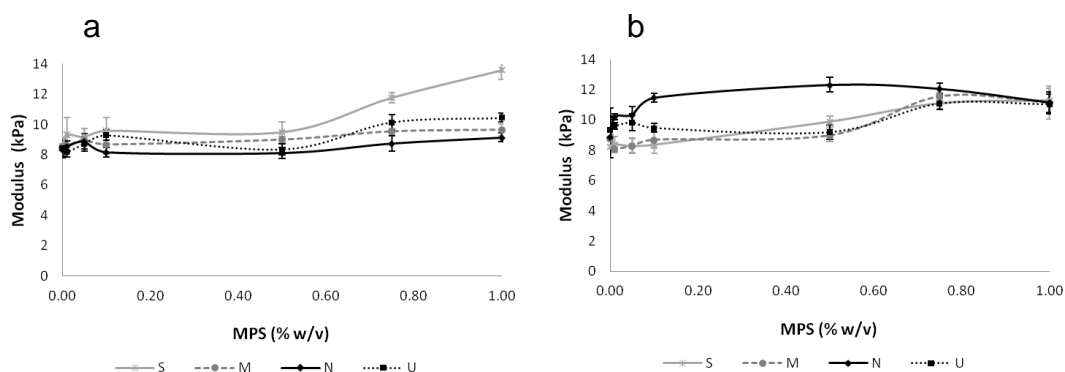


FIGURE 5. Effect of MSP concentration on the Young's Modulus of gelatine gels. a) Non-functionalised MSP. b) Functionalised MSP. SBA-15 (S), Microparticulated MCM-41 (M), Nanoparticulated MCM-41 (N) and UVM-7 (U).

Functionalised and non-functionalised MSP can be considered active fillers since active fillers are molecules able to bind to the matrix and increase the gel modulus (Sala et al., 2007). This interaction can be explained by the presence of silanol groups in non-functionalised particles and amino groups in functionalised particles, which are able to interact with amino and carboxylic groups of the gelatine (Coradin, 2004). When the filler and the polymer interact, a restriction on the mobility and a deformation of the matrix is induced, generating a mechanical restraint. The contribution to the mechanical restraint depends on the properties of the particle and the matrix.

There are three decisive factors determining the elastic modulus of a filler-polymer composite: the elastic modulus of the filler and the matrix (the higher the elastic modulus of the filler, the higher the elastic modulus of the composite), the filler concentration and the aspect ratio of the filler (Fu et al., 2008). In this case, the improvement experienced by the gelatine gels as a result of the addition of different concentrations is the result of the three mechanisms previously described. First, the Young's modulus of SiO_2 , much higher than that of the gelatine, augmented the elastic modulus of the gel; second, the increase of MSP concentration provoke a raise in the Young's Modulus, being this behaviour congruent with previous literature (Chrissafis et al., 2007); third, the different aspect ratio of the four MSP justifies their different contribution to the increase of the Young's modulus.

Fracture stress (parameter related with strength) of the different gels is plotted in Figure 6. In gels, the increase of the strength is deeply related with particle-polymer interaction. For both, non-functionalised and functionalised MSP, a potential interaction from the particle with the protein chain of the gelatine, with its consequent increase on the gel strength, was expected. On the one hand, silicate species (as those present in non-functionalised MSP) have shown to interact through both electrostatic interactions and hydrogen bonding with some poly-aminoacids and proteins (Coradin et al., 2004; Fernandes et al., 2011). On the other hand, amine functionalised-nanoparticles have also shown to interact with a large amount of proteins (Lunqvist et. al, 2008).

However, as shown in Figure 6, the incorporation of non-functionalised MSP did not exhibit an increase on fracture stress, in contrast with the addition of functionalised MSP, which showed a remarkable increase for concentrations above 0.5%.

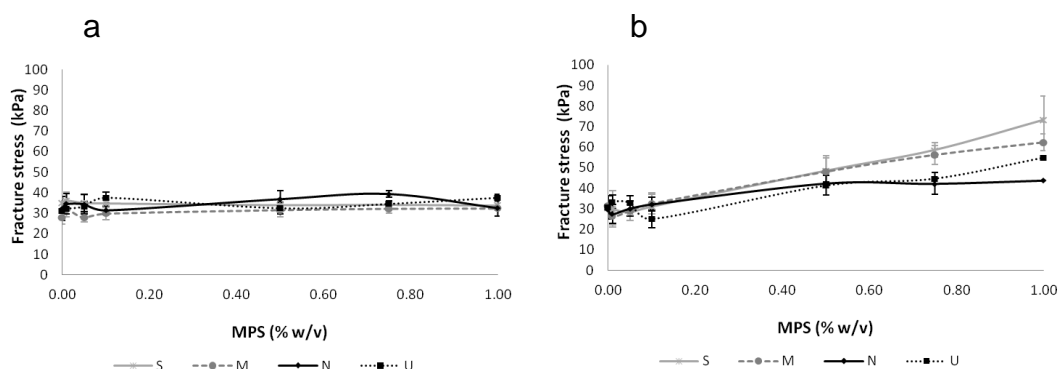


FIGURE 6. Effect of MSP concentration on Fracture Stress of gelatine gels. a) Non-functionalised MSP. b) Functionalised MSP. SBA-15 (S), Microparticulated MCM-41 (M), Nanoparticulated MCM-41 (N) and UVM-7 (U).

Making a deeper analysis of the phenomena that govern the structure of a filled gel it is found that not only the polymeric matrix and the fillers have an impact on the properties of the gel, but also the interfacial area. The interfacial area refers to the zone that surrounds the particles, a layer consisting of immobilized polymer whose structure and properties change because of the interaction with the particle, making it different from the rest of the matrix (See scheme in Figure 7a). Stronger interactions between the particle and the polymer leads to an improvement of the interfacial area and thus on the mechanical properties of the gel (Pitsa and Danikas, 2011).

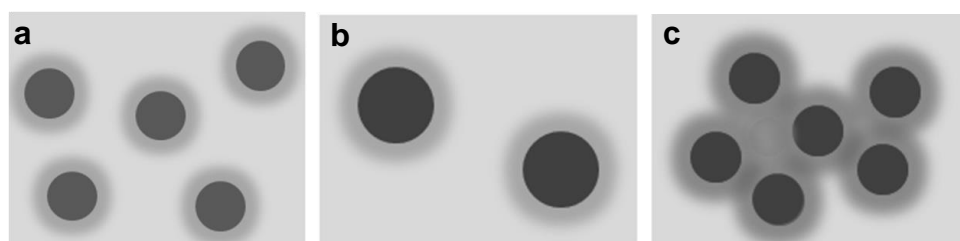


FIGURE 7. a) Scheme of the structure of a filled gel: polymeric matrix (light grey zone), fillers (black spheres) and the interfacial area (dark layers surrounding the particles). b) Interfacial area formation under low concentration of particles (large distance between interfacial areas). c) Interfacial area formation under high concentration of particles (overlap of interfacial areas, increase of bounding between layers).

According to this phenomenon, the increase of strength observed with the incorporation of functionalised MSP was due to strong interactions with the polymeric chain, which resulted in a strong interfacial area. This effect is also congruent with literature, which states that through the incorporation of organic moieties on nanoparticles, the compatibility between the inorganic nanoparticles and the polymer matrix is improved, affecting positively the stability and specific surface of the interfacial area (Pitsa and Danikas, 2011; Tjong, 2006).

For well-bonded particles with strong interfacial area, the stress applied to the matrix can be effectively transferred from the matrix to the particles, clearly improving the gel strength (Fu et al., 2008).

This strong interaction, however, could not be present on non-functionalised MSP as a consequence of the aggregation. As mentioned before, non-functionalised MSP had zeta potential values within the instability zone and had a marked tendency to form particle aggregates (see Table 2). Some studies also confirmed that silicates under acidic pH conditions do not present an effective interaction with the polymeric matrix, and go under aggregation instead (Coradin et al., 2004). Large aggregates of non-functionalised MSP could introduce defect centres in the matrix, acting like weak point (stress concentrators) from which a fracture can occur (Pitsa and Danikas, 2011; Fernandes et al., 2011) and consequently having no positive effects on gel strength.

Figure 6b displays some additional information. First, it shows that there is a remarkable dependence of particle concentration and gel strength, since a significant increase was observed only for concentrations above 0.5%. Second, it also reveals that small size particles (SBA-15 and Microparticulated MCM-41) had a more pronounced increase than large size particles (Nanoparticulated MCM-41 and UVM-7). The impact of particle size and concentration can be explained as follows. Large size particles and low concentration will result in a low number of particles embedded in the matrix. At low number of particles, the distance between them is too large and the interfacial area of each particle remains isolated from the rest (See Figure 7b). For small size particles and high concentration, the number of particles increases, and the interfacial areas of each particle begin to overlap, resulting in an intensification of the interactions (see Figure 7c) (Vaia and Wagner, 2004).

Figure 8 shows the effect of MSP concentration on fracture strain (parameter related to brittleness) of the gelatine gels. It can be seen that no significant differences were found associated with the addition of the non-functionalised MSP. Functionalised MSP instead exhibited a slight increase on the fracture strain of the gels, resulting in less brittle gels.

This result is consistent with other studies that have showed to significantly improve the strain at break of polymers by the incorporation of hybrid nanofillers (inorganic nanoparticles with organic surface) (Tjong, 2006). This improvement is also related to a better filler-matrix interaction, increasing the integrity and stability of the gel and thus making it stand more deformation before going into fracture.

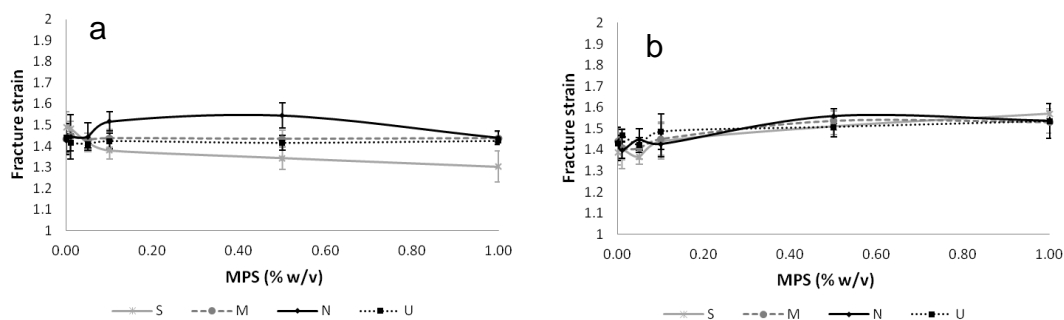


FIGURE 8. Effect of MSP concentration on fracture strain of the gelatine gels. a) Non-functionalised MSP. b) Functionalised MSP. SBA-15 (S), Microparticulated MCM-41 (M), Nanoparticulated MCM-41 (N) and UVM-7 (U).

CONCLUSIONS

Five different MSP were synthesised, functionalised and incorporated into a gelatine matrix. Characterisation analysis of the MSP showed evident differences in morphology, size and zeta potential of the particles. Functionalisation showed to have a significant impact in the size, charge and stability of the MSP. The presence of MSP increased the turbidity of the gelatine gels, being the effect conditioned not only by the concentration of the particle, but also by its size. The incorporation of MSP showed an increase in Young's modulus of the gelatine gels in all cases. A remarkable increase on the strength and a slight reduction on the brittleness of the gels were observed from the addition of functionalised MSP while non-functionalised MSP showed no effect on these mechanical properties. Size, morphology, charge, stability and concentration of the MSP have proven to have a decisive impact on the turbidity and mechanical properties of the gelatine gels.

ACKNOWLEDGEMENTS

I would like to thank Dr. José Manuel Barat for his thoughtful insights. I also would like to express my very great appreciation to Ph.D student Edgar Perez for his guidance, encouragement and resolute dedication to support this study. My special gratitude to Katarzyna Sopol, Agnieszka Kasperek and Rafael Casillas for their assistance during the experimental work.

I would like to thank my family as well for giving me the courage to undertake this and every challenge. I am particularly grateful to Alfredo Santos whose patience, love and humour have given me the strength to go through this journey. Finally, though they cannot possibly know how much of an inspiration they have been, I would like to thank Nieves and Chantilly.

REFERENCES

- Agostini, A.; Sancenón, F.; Martínez-Mañez, R.; Marcos, M.D.; Soto, J. & Amorós, P. (2012) A photoactivated molecular gate. *Chemistry*. 18: 12218-12221.
- Akihiro, T.; Baiju, J.; Arakawa, S. & Okatamo, M. (2013). Structure and rheology of nanocomposite hydrogels composed of DNA and clay. *European Polymer Journal*. 49: 923-931.
- Barat, J. M.; Pérez-Esteve, E.; Bernardos, A. & Martínez-Mañez, R. (2011). Nutritional effects of folic acid controlled release from mesoporous materials. *Procedia Food Science*. 1(0): 1828-1832.
- Benhamou, A.; Basly, J.P.; Baudu, M.; Derriche, Z & Hamacha, R. (2013). Amino-functionalised MCM-41 and MCM-48 for the removal of chromate and arsenate. *Journal of Colloid and Interface Science*. 404: 135–139
- Bernardos, A.; Aznar, E.; Coll, C.; Martínez-Mañez, R.; Barat, J.; Marcos, M.; Sancenón, F.; Benito, A. & Soto, J. (2008). Controlled release of vitamin B2 using mesoporous materials functionalised with amine-bearing gate-like scaffolds. *Journal of Controlled Release*. 131: 181-189.
- Bernardos, A.; Mondragón, L.; Aznar, E.; Marcos, M.D.; Martínez-Mañez, R.; Sancenón, F.; Soto, J.; Barat, J.M.; Pérez-Payá, E.; Guillem, C. & Amorós, P. (2011). Enzyme-responsive intracellular controlled release using nanometric silica mesoporous supports capped with 'saccharides'. *ACS nano*. 4(11):6353-6368.
- Cabero, M.; Hungría, A.; Morales, J.; Tortajada, M.; Ramón, D.; Moragues, A.; Haskouri, J.; Beltrán, A.; Beltrán & Amorós, P. (2012). Interconnected mesopores and high accessibility in UVM-7-like silicas. *J Nanopart Res*. 14:1045-1057.
- Charnay, C., Bégu, S., Tourné-Péteilh, C., Nicole, L., Lerner, D. A. & Devoiselle, J. M. (2004). Inclusion of ibuprofen in mesoporous templated silica: drug loading and release property. *European Journal of Pharmaceutics and Biopharmaceutics*. 57(3): 533–540.
- Chrissafis, K.; Antoniadis, G.; Paraskevopoulos, K.; Vassiliou, A. & Vikiaris, D. (2007). Comparative study of the effect of different nanoparticles on the mechanical properties and thermal degradation mechanism of in situ prepared poly(ϵ -caprolactone) nanocomposites. *Composites Science and Technology*. 67: 2165–2174.
- Climent, E., Bernardos, A., Martínez-Mañez, R., Maquieira, A., Marcos, M.D., Pastor-Navarro, N., Puchades, R., Sancenón, F., Soto, J. & Amorós, P. (2009). Controlled delivery systems using antibody-capped mesoporous nanocontainers. *Journal of the American Chemical Society*. 131(39):14075-14080.
- Comes, M., Aznar, E., Moragues, M., Marcos, M. D., Martínez-Mañez, R., Sancenón, F., Soto, J., Villaescusa, L.A., Gil, L. & Amorós, P. (2009) Mesoporous hybrid materials containing nanoscopic "binding pockets" for colorimetric anion signaling in water by using displacement assays. *Chemistry A European Journal*. 15(36): 9024-9033.
- Coradin, T., Bah, S. & Livage, J. (2004) Gelatine/silicate interactions: from nanoparticles to composite gels. *Colloids and Surfaces B: Biointerfaces*. 35:53-58
- Fernandes, F.; Manjubala, I.; Ruiz-Hitzky, E. (2011). Gelatin renaturation and the interfacial role of fillers in bionanocomposites. *Phys. Chem. Chem. Phys*. 13: 4901–4910.
- Fu, S.; Feng, X; Lauke, B. & Mai, J. (2008). Effects of particle size, particle/matrix interface adhesion and particle loading on mechanical properties of particulate–polymer composites. *Composites: Part B*. 39: 933–961.
- Gregory, J. (1998). Turbidity and Beyond. *Filtration and Separation*. 63-67
- Haranath, D.; Gandhi, N.; Sahai, S.; Husain, M. and Shanker, V. Highly emissive and low refractive index layers from doped silica nanospheres for solar cell applications. (2010). *Chemical Physics Letters*. 496: 100-103.
- Horcajada, P.; Rámila, A.; Pérez-Pariente, J. & Vallet-Regí, M. Influence of pore size of MCM-41 Matrices on Drug Delivery Rate. *Micropor. Mesopor. Mat*. 68:105-109.
- Innocenzi, P & Malfatti, L. (2013). Mesoporous thin films: properties and applications. *Chem Soc. Review*. 42: 4198-4216.
- Jaganathan, H. & Godin, B. (2012). Biocompatibility assessment of Si-based nano- and micro- particles. *Advanced Drug Delivery Reviews*. 64:1800–1819.
- Kharim, A. A. & Bhat, R. (2008) Gelatin alternatives for the food industry: recent developments, challenges and prospects. *Trends in Food Science & Technology* 19: 644-656
- Kuijpers, A. J., Engers, G. H. M., Feijen, J., De Smedt, S. C., Meyvis, T. K. L., Demeester, J., Krijgsveld, J., Zaat, S. A. J., Dankert, J. (1999) *Macromolecules*. 32: 3325–3333.

- Lau, M., Tang, J., Paulson, A. (2000). Texture profile and turbidity of gellan/gelatin mixed gels. *Food Research International*. 33: 665-671.
- Lee, K., Shim, J., Young, I., Cha, J., Seok, C. and Gyu, H. (2003). Characterisation of gellan/gelatin mixed solutions and gels. *Lebensm.-Wiss. U.-Technol.* 36: 795-802
- Lunqvist, M.; Stigler, J.; Elia, G.; Lynch, I.; Cedervall, T. & Dawson, K. (2008). Nanoparticle size and surface properties determine the protein corona with possible implication for biological impacts. *PNAS*. 105 (38): 14265-14270.
- Mamaeva, V., Sahlgren, C. and Lindén, M. (2013). Mesoporous silica nanoparticles in medicine—Recent advances. *Advanced Drug Delivery Reviews*. 65: 689-702
- Maruo, T.; Tanaka, S.; Nishiyama, N.; Motoda, Ken.; Funayama, K.; Egashira, Y. & Ueyama, K. Low-index mesoporous silica films modified with trimethylethoxysilane. *Colloids and Surfaces A: Physicochem. Eng. Aspects*. 318:84–87.
- Nandiyanto, A., Kim, S., Iskandar, F. and Okuyama, K. (2009). Synthesis of spherical mesoporous silica nanoparticles with nanometer-size controllable pores and outer diameters. *Japan Microporous and Mesoporous Materials*. 120: 447-453
- Peleg, M. (1987). The basics of solid foods rheology. In Moskowitz, H. R., *Food texture - Instrumental and sensory measurements*. (pp. 3-33). New York: Marcel Dekker.
- Pérez-Esteve, E., Bernardos, A., Martínez-Mánez, R., Barat, J. M. (2013). Nanotechnology in the Development of Novel Functional Foods or their Package. An Overview Based in Patent Analysis. *Recent Patents on Food, Nutrition & Agriculture*. 4(3):172-178.
- Pitsa, D. & Danikas, M. (2011). Interfaces Features in Polymer Nanocomposites: A review of proposed models. *NANO: Brief Reports and Reviews*. 6 (6): 497-508.
- Rouquerol, J., Avnir, D., Fairbridge, W., Everett, D., Haynes, J., Pernicone, N., et al. (1994). Recommendations for the characterization of porous solids (Technical Report). *Pure & Appl. Chem*. 66 (8): 1739-1758.
- Sala, G.; Van, G.; Cohen, M. and Van, F. (2007). Effect of droplet-matrix interactions on large deformations properties of emulsion-filled gels. *Journal of Texture Studies*. 38:511-535.
- Sala, G.; Van Vliet, T.; Cohen, M.; van Aken, G. And van de Velde, F. (2009). Deformation and fracture of emulsion-filled gels: Effect of oil content and deformation speed. *Food Hydrocolloids*. 23: 1381-1393.
- Shubbert, E.; Kim, J. & Xi, J. (2007). Low-refractive-index materials: A new class of optical thin-film materials. *Phys. stat. sol.* 244(8):3002-3008.
- Trewyn, B., Giri, S. and Slowing, I. (2007). Mesoporous silica nanoparticle based controlled release, drug delivery and biosensor systems. *Chem. Commun.* 3236-3245.
- Tjong, S. (2006). Structural and mechanical properties of polymer nanocomposites. *Materials Science and Engineering R*. 53: 73–197
- Vaia, R. & Wagner, D. (2004). Framework for nanocomposites. *Materials today*. 32-37.
- Vallet-Regí, M., Doadrio, J., Doadrio, A., Izquierdo-Barba, I. and Pérez-Pariente, J. (2004). Hexagonal ordered mesoporous material as a matrix for the controlled release of amoxicillin. *Solid State Ionics*. 172(1–4): 435–439.
- Vallet-Regí, M., Balas, F. and Arcos, D. (2007). Mesoporous Materials for Drug Delivery. *Angew. Chem. Int.* 46: 7548-7558.
- Van Vliet, T., van Aken, G. A., de Jongh, H. H. & Hamer, R. J. (2009) Colloidal aspects of texture perception. *Advances in Colloid and Interface Science*. 150(1): 27-40
- Xu, Z., Ji, Y., Guan, M., Huang, H., Zhao, C. & Zhang, H. (2010) Preparation and characterisation of L-Leucine-modified amphiprotic bifunctional mesoporous SBA-15 molecular sieve as a drug carrier for ribavirin. *Applied Surface Science* 256(10): 3160-3165
- Yang, Y., Anvari, M., Pan, C. & Chung, D. (2012). Characterisation of interactions between fish gelatin and gum arabic in aqueous solutions. *Food Chemistry*. 135: 555-561.
- Zhao, D., Q. Huo, J. Feng, B.F. Chmelka and G.D. Stucky, 1998b. Nonionic triblock and star diblock copolymer and oligomeric surfactant syntheses of highly ordered, hydrothermally stable, mesoporous silica structures. *J. Am. Chem. Soc.* 120: 6024-6036